

Journal of Biomedical Optics

BiomedicalOptics.SPIEDigitalLibrary.org

Shortwave-infrared Raman spectroscopic classification of water fractions in articular cartilage *ex vivo*

Mustafa Unal
Ozan Akkus

Shortwave-infrared Raman spectroscopic classification of water fractions in articular cartilage *ex vivo*

Mustafa Unal^{a,b,†} and Ozan Akkus^{a,b,c,d,*}

^aCase Western Reserve University, Department of Mechanical and Aerospace Engineering, Cleveland, Ohio, United States

^bCase Western Reserve University, Center for Applied Raman Spectroscopy, Cleveland, Ohio, United States

^cCase Western Reserve University, Department of Orthopaedics, Cleveland, Ohio, United States

^dCase Western Reserve University, Department of Biomedical Engineering, Cleveland, Ohio, United States

Abstract. Water loss is an early onset indicator of osteoarthritis. Although Raman spectroscopy (RS) holds the potential for measurement of cartilage hydration, the knowledge of Raman OH-stretch bands of biological tissue is very limited. We assessed here the sensitivity of RS to identify and classify water types in the cartilage. Raman spectrum measurements over the high wavenumber range were employed to identify different water fractions in articular cartilage. Raman spectra were collected from wet and sequentially dehydrated cartilage along with pure collagen type II and chondroitin sulfate standards. OH-stretch band of cartilage is dominated by mobile water, up to 95% of total intensities. We identified six peaks in cartilage spectrum using second-derivative analysis: peaks at 3200 and 3650 cm^{-1} are associated with organic matrix (both collagen and proteoglycan) and matrix-bound water molecules. Peaks at 3250, 3453, and 3630 cm^{-1} are associated with collagen and collagen-related water molecules, whereas the peak at 3520 cm^{-1} is associated with proteoglycan (PG) and PG-related water molecules. The current work is the first thorough analysis of the Raman OH-stretch band of the cartilage and with the knowledge generated by this study, it may now be possible to study on cartilage hydration by RS. © 2018 Society of Photo-Optical Instrumentation Engineers (SPIE) [DOI: 10.1117/1.JBO.23.1.015008]

Keywords: cartilage; Raman spectroscopy; OH stretch band; bound water; collagen; proteoglycan; osteoarthritis.

Paper 170695R received Oct. 26, 2017; accepted for publication Jan. 4, 2018; published online Jan. 26, 2018.

1 Introduction

Osteoarthritis (OA) is a debilitating musculoskeletal disease characterized by degeneration of articular cartilage¹ and has been recognized as one of the fastest growing diseases worldwide because of increased prevalence of obesity and aging of the society.² Since cartilage has a limited ability for self-repair, it is crucial to detect early stage of OA to increase the success of treatment. Therefore, a great amount of effort has been focused on developing a reliable noninvasive and nondestructive method to probe the pathogenesis of the earliest stages of OA. Early stage of OA is characterized by a damaged collagen network, loss of proteoglycans (PGs), and an increase in water content by up to 10% to 15%.^{3–8} These early changes in the cartilage cannot be detected using traditional clinical methods such as radiography or arthroscopy. Therefore, any technique that is sensitive and specific to these early changes is valuable for early detection of OA.

Recent years have shown that measurement of water content in the cartilage holds a great potential for early detection of OA.⁹ Furthermore, water is the critical component to physiological and mechanical functions of cartilage.¹⁰ Therefore, water is an ideal biomarker to study on cartilage quality. However, there is a dearth of nondestructive methods for assessing hydration status of cartilage. Magnetic resonance imaging (MRI)-based methods are among the few available nondestructive methods for analyzing water content in cartilage;⁹ however,

the sensitivity of MRI analyses to detect very small changes in water content (~10%) in early stages of OA is limited due to limited spatial resolution and the partial-volume averaging effects.^{11,12} Near-infrared (NIR) spectroscopy is an emerging method to assess hydration status of cartilage.¹³ However, bands in the NIR spectrum are typically very broad, leading to spectra that are chemically less specific and hard to interpret. Thus, developing a new nondestructive method for spatially assessing hydration status of cartilage is a potentially useful step toward investigating the role of water in cartilage quality.

Raman spectroscopy (RS) has become a powerful nondestructive and label-free technique to assess biochemical changes in the cartilage due to diseases, aging and mechanical loading.^{14–18} Unlike other vibrational spectroscopic techniques (FTIR, MIR, and NIR), RS has nondestructive and noninvasive clinical feasibility in the near term when employed in the spatially offset or transmission mode.¹⁹ As described in a recent review by Matousek and Stone,¹⁹ a number of studies have showed that spatially offset RS and transmission RS are emerging fields in *in vivo* diagnosis of several diseases including bone disorder and breast cancer or tomographic imaging of biological tissues. Thus, RS also holds potential to assess hydration status of cartilage *in vivo*. However, to date, RS technique has been limited to investigate only the lower wavelength region of the cartilage spectrum in the range of 800 to 1800 cm^{-1} . This fingerprint region is dominated by collagen and PG-related peaks and provides little information on water. On the other hand, the higher wavenumber region of the spectrum between 2700 and 3800 cm^{-1} , where CH, OH, and NH stretch bands are

*Address all correspondence to: Ozan Akkus, E-mail: ozan.akkus@case.edu

[†]Current affiliation: Vanderbilt University Medical Center, Department of Orthopaedic Surgery and Rehabilitation, Nashville, Tennessee, United States

located in the target region for understanding the hydration of cartilage. Study of high wavenumber range is largely impeded by lack of sensitivity of charged coupled detectors (CCDs) in this region. High wavenumber RS has been previously used to measure water content in several biological tissues, including skin,^{20,21} nails,^{20,22} hair,²⁰ cornea,^{23,24} and bone.^{25–29} However, to the best of our knowledge, RS has not been used to study on hydration status of cartilage and OH-stretch subpeaks of cartilage have not been related to varying water fractions in the cartilage. Therefore, to begin addressing the potential of RS to assess hydration status of the cartilage, we embarked to identify water-associated Raman signatures in the cartilage.

2 Materials and Methods

2.1 Cartilage Specimen Preparation

Cartilage plugs with full thickness (~1 to 2 mm) were excised from two fresh mature bovine knee joints using a scalpel and a 4-mm diameter biopsy punch. The articular cartilage plugs ($N = 6$) were then stored frozen at -20°C until use.

To tease out PG and collagen type II contributions to the OH band, Raman spectra of chondroitin sulfate (CS) powder (Sigma-Aldrich, St. Louis, Missouri) and collagen type II from calf joints (Elastin Products Company, Owensville, Missouri) were recorded from both intact and gradually hydrated specimens. Briefly, these specimens were placed on an aluminum slide and Raman spectra were collected at room temperature. Then, these specimens were gradually hydrated until they reached fully hydrated state (no water absorbed anymore by the specimens). Raman spectra were simultaneously collected during the progressive hydration.

2.2 Serial Dehydration and Gravimetric Measurements

The full depth plugs of cartilage were allowed to equilibrate at room temperature in phosphate buffered saline. Superficial water on specimen surface was gently blotted and wet weight of specimens was measured (Model XS64, Mettler Toledo, Columbus, Ohio). The specimens were then left at room temperature in air for 60 min and weighed again. Following air drying, the specimens were heated in an incubator in air at a rate of $\sim 15^{\circ}\text{C}$ per minute, held at 37°C for 48 h, and weighed again. The treatment duration was chosen because specimen weights did not change for longer durations. The temperature was selected to stay below the denaturation temperature of organic matrix macromolecules (i.e., collagen and PG) around 50°C to 70°C .^{30,31} The oven drying conditions are, therefore, expected to remove predominantly mobile water and have minimal effect on tightly bound water compartment, which requires much higher temperature to remove from the matrix.^{30,31}

The specimens were kept in a sealed plastic bag except when gravimetric and Raman analyses were carried out to avoid rehydration by the moisture in air. The percent water loss was calculated as

$$\text{Water loss \% by weight} = 100 \times (W_w - W_d) / W_w, \quad (1)$$

where W_w is the initial wet weight of cartilage, and W_d is the weight after each dehydration step. In parallel with gravimetric measurements, Raman spectra of specimens were collected immediately after each drying/treatment episode.

2.3 Hydrogen–Deuterium (H/D) Exchange

The long-term deuterium exchange beyond oven drying provides information on the rate of dissociation of different moieties of bound water through observation of the disappearance of OH-related Raman peaks.²⁷ Thus, a group of cartilage specimens dried in an oven were immersed into 1 ml of deuterium oxide (D_2O , 99.9% isotopic purity, Sigma-Aldrich., St. Louis, Missouri) for 60 min, 24 h, and 7 days,²⁷ with periodic replacement of D_2O at room temperature. Raman spectra were collected immediately after each step of deuterium treatment.

2.4 Shortwave-Infrared Raman Spectroscopy and Data Processing

Quantum efficiency of the CCDs of standard 785-nm Raman systems decline in the higher wavenumber OH-stretch range; therefore, a refined analysis of the water compartments in biological tissues is challenging with standard RS when using with near-infrared laser wavelength. We recently customized a SWIR-RS system^{25,27} to survey the OH-stretch range of biological tissues while accommodating the protein-related background fluorescence. Our SWIR-RS has been previously described in detail.^{25–27} Briefly, this SWIR-RS system involved excitation at 847 nm (Axcel Photonics) and signal collection using a short-wave InGaAs IR spectrometer (BaySpec, Inc., California) specifically optimized for 1000- to 1400-nm wavenumber range that provided data collection in a spectral range of ~ 2550 to 4770 cm^{-1} , which covered the CH and OH-stretch bands sufficiently.

Measurement locations at the articular surface were positioned equidistantly to cover the region of interest and Raman spectra were collected from the same location at a $100\text{-}\mu\text{m}$ laser spot size. Signal collection time was set at 10 s with an accumulation of 10 scans. Laser power was set to $\sim 25\text{ mW}$ on the sample to avoid possible water loss and cartilage matrix damage associated with excessive laser heating.³² Representative spectra for any given treatment condition were obtained by taking the average of three spectra collected from each six cartilage specimens at room temperature. Raman spectra were analyzed using LabSpec 5 (Horiba Scientific, Edison, New Jersey) and OriginLab (OriginLab Corporation, Northampton, Massachusetts) softwares to determine the position and intensity of the peaks. The background was removed by subtracting the fitted fluorescence baseline from the raw spectra using piecewise linear segments. Then, the averaged spectra were smoothed to improve signal-to-noise ratio via denoising algorithm of LabSpec 5 software. The spectra were then fitted through second-derivative analysis to identify peak locations. All spectra were normalized to attain the same intensity for the CH-stretch band that is emerging from the organic matrix. Therefore, band intensity values reported in this study are normalized to total amount of organic matrix in the cartilage specimens.

2.5 Statistical Analysis

All statistical analyses were performed using Minitab 16 statistical software (Minitab, Inc., State College, Pennsylvania). Data were presented as mean \pm standard deviation. Linear regression analyses were performed between Raman peak intensities versus gravimetrically measured water loss during progressive

dehydration. Statistical significance was considered at a p -value <0.05 for the resulting R^2 value.

3 Results

3.1 Determination of Peak Locations in OH-Stretch Band of Wet Cartilage and Bulk Water

The presented spectra result from the average of 18 Raman spectra taken at different locations from six cartilage specimens. The standard deviation was within %13 of the intensity. All cartilage spectra in this study are scaled to obtain the same intensity at the CH-stretch peak centered at $\sim 2930\text{ cm}^{-1}$ [Fig. 1(a)]. The wavenumber range of 2700 to 3050 cm^{-1} manifests CH-stretch band associated with collagen and PG phases of cartilage matrix, whereas OH-stretch band extends across 3100 to 3800 cm^{-1} .

The comparison of Raman spectra of cartilage specimens with bulk water is shown in Fig. 1(a). OH-bands of fully hydrated cartilage spectrum and bulk water displayed prominent peaks at ~ 3250 and $\sim 3450\text{ cm}^{-1}$, with the former peak being more pronounced for bulk water [Fig. 1(a)]. A direct comparison of Raman spectrum of bulk water with wet and oven-dried cartilage specimens indicated the prominence of mobile water-related Raman intensity in wet cartilage [Fig. 1(a)]. Raman difference spectrum calculated by subtracting the spectrum of wet cartilage from oven-dried cartilage specimens confirmed that mobile water fraction accounted for about 95% of the Raman intensities of wet cartilage [Fig. 1(c)].

Using second-derivative method, locations of six peaks (three central peaks with their three shoulders) in OH-stretch bands of wet cartilage were revealed [Table 1 and Fig. 1(b)]. For wet cartilage, central peaks are located at ~ 3200 , ~ 3450 , and $\sim 3630\text{ cm}^{-1}$ and their shoulders at ~ 3250 , ~ 3520 , and $\sim 3650\text{ cm}^{-1}$, respectively. For bulk water, there were five peaks located at ~ 3015 , ~ 3220 , ~ 3410 , ~ 3565 , and 3630 cm^{-1} , respectively [Table 1 and Fig. 1(b)]. The changes in intensities of major cartilage peaks were significantly correlated with the gravimetric water loss obtained by subtracting wet weight from oven-dried weight [Fig. 1(d)], indicating these Raman peaks were sensitive to dehydration and were associated with water content in cartilage.

3.2 Changes in OH-Stretch Band of Cartilage Under Sequential Dehydration

There was a stepwise decline in the Raman intensities of cartilage's OH-stretch band upon sequential drying [Fig. 2(a)]. We observed the peak intensities to stabilize after 48 h of oven drying, and the changes in peak intensities were significantly correlated with the gravimetric water loss [Fig. 1(d)].

The comparison of second-derivative Raman spectra of wet cartilage with oven-dried cartilage specimens showed that the observed locations of peaks and shoulders in wet cartilage shifted to lower or higher frequencies [Figs. 1(b) and 2(b)]. Following oven drying, a peak centered at $\sim 3330\text{ cm}^{-1}$ was revealed, which is likely to be associated with NH-stretching

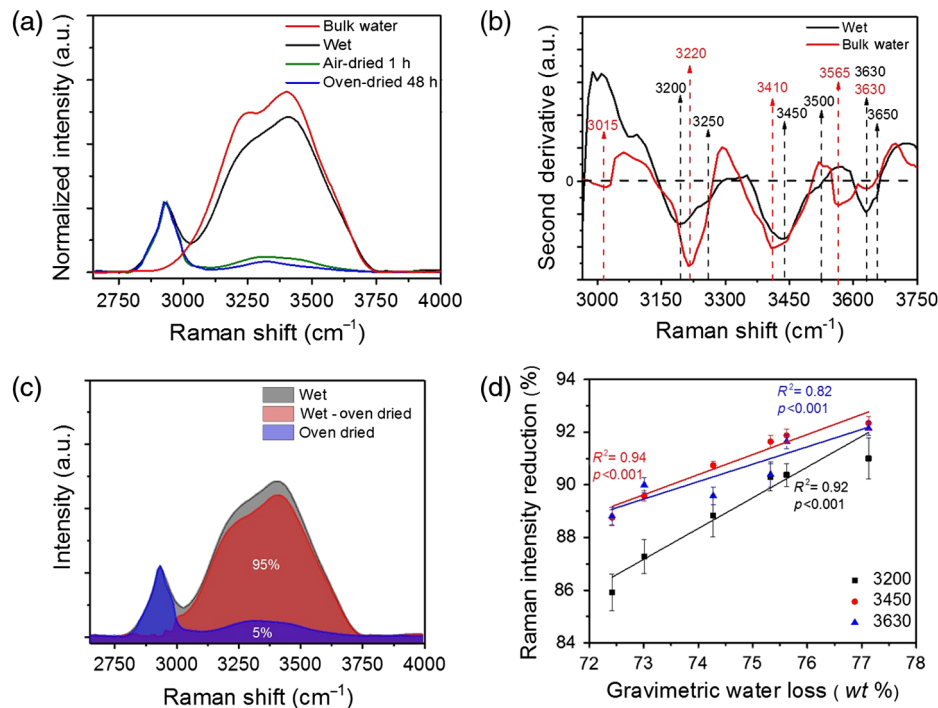
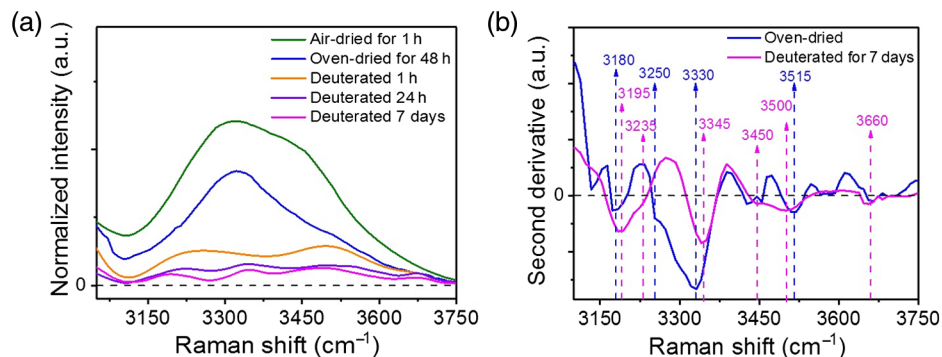


Fig. 1 Raman OH stretch band of cartilage. Cartilage spectra are normalized with respect to the CH-stretch intensity that is representing the amount of protein. (a) Raman intensity changes of wet cartilage during sequential dehydration in the ambient for up to 60 min and in an oven for 48 h along with the Raman spectra of bulk water. The standard deviation is within 13% of the intensity and not shown in the spectra for the sake of clarity. (b) Second derivative spectra of wet cartilage and bulk water. Red dashed line indicates bulk water-related peaks and black dashed line indicated wet cartilage related peaks. (c) OH band of wet and oven-dried cartilage and their difference spectra, showing predominance of mobile like water. (d) R^2 for pairwise correlations between water loss measured by central three OH peaks and water loss by weight. All correlations are significant at $p < 0.05$.

Table 1 Raman band assignments and origin of the subpeaks. DAA-OH, single donor–double acceptor; DDAA-OH, double donor–double acceptor; DA-OH, single donor–single acceptor; DDA-OH, double donor–single acceptor; PG, proteoglycan; collagen: collagen type II; water, bound and mobile water.

Samples	Wavenumbers (cm ⁻¹)	Vibration mode	Hydrogen-bonding type	Assignment (origin of the peak)
Bulk water	~3015	OH symmetric stretch band	DAA-OH	Water
	~3220	OH symmetric stretch band	DDAA-OH	Water
	~3410	OH-asymmetric stretch band	DA-OH	Water
	~3565	OH-asymmetric stretch band	DDA-OH	Water
	~3630	Nonhydrogen OH band	Free-OH (dangling)	Water
Wet cartilage	~3200	OH symmetric stretch band	DDAA-OH	Water, collagen, PG
	~3250	OH symmetric stretch band	DDAA-OH	Water, collagen
	~3450	OH-asymmetric stretch band	DA-OH	Water, collagen
	~3520	OH-asymmetric stretch band	DDA-OH	Water, PG
	~3630	Nonhydrogen OH band	Free-OH (dangling)	Water, collagen
	~3650	Nonhydrogen OH band	Free-OH (dangling)	Water, collagen, PG
Deuterated cartilage	~3195	OH symmetric stretch	DDAA-OH	Collagen, PG
	~3235	OH symmetric stretch	DDAA-OH	Collagen
	~3345	NH stretch band	NH + DA-OH	Collagen, PG
	~3450	OH-asymmetric stretch band	DA-OH	Collagen
	~3500	OH-asymmetric stretch band	DDA-OH	PG
	~3660	Nonhydrogen OH band	Free-OH (dangling)	Collagen, PG

**Fig. 2** Raman OH stretching bands of deuterium oxide-treated specimens. (a) OH intensity change in dehydrated cartilage due to progressive deuterium oxide treatment. The standard deviation is within 13% of the intensity and not shown in the spectra for the sake of clarity. (b) Second derivative spectra of oven-dried and deuterated cartilage. Pink dashed lines indicate OH peaks associated with macromolecules of collagen and PG. Blue dashed lines indicate OH peaks associated with mainly bound water molecules.

band along with tightly bound water since it is also sensitive to deuterium oxide treatment [Fig. 2(a)].

Spectral changes associated with bound water were revealed by Raman spectra of oven-dried cartilage specimens under H/D exchange treatment [Fig. 2(a)]. Comparison of deuterated spectra with spectra from oven-dried samples indicated Raman signal after oven drying was associated mainly with bound water compartments, which accounted for 3 to 4% of the total Raman intensities along with the contributions of organic matrix

[Fig. 2(a) and Table 2]. We observed that Raman intensities stabilized upon 7 days long H/D exchange treatment, indicating there is no water fractions left in the matrix.²⁷ The second-derivative analysis showed the locations of six peaks in OH-stretch bands of deuterated cartilage specimens (Table 1) at ~3195, ~3235, ~3345, ~3450, ~3500, and ~3660 cm⁻¹, respectively [Fig. 2(b) and Table 1], and should be associated with the organic matrix of cartilage that is left after deuteration of water molecules.

Table 2 The breakdown of band intensities in wet cartilage between mobile water, bound water, and cartilage matrix.

Peak location (cm ⁻¹)	Mobile water (%) ^a	Bound water (%) ^b	Matrix (%) ^c
~3200	95.24 ± 1.85	3.20 ± 1.05	1.56 ± 0.62
~3250	93.96 ± 2.28	4.59 ± 1.62	1.45 ± 0.98
~3450	95.93 ± 1.41	2.48 ± 1.33	1.59 ± 0.43
~3520	95.77 ± 1.80	2.32 ± 1.29	1.91 ± 0.63
~3630	95.87 ± 2.52	0.97 ± 0.75	3.16 ± 0.56
~3650	94.53 ± 5.00	1.04 ± 1.29	4.43 ± 0.71

^aIntensity reduction following air and oven drying.

^bIntensity reduction following deuterium treatment for 7 days.

^cRemnant intensity due to collagen backbone (amide A), hydroxyproline, or PGs.

3.3 Raman High-Wavenumber Spectra of Pure Collagen Type II and Chondroitin Sulfate

Raman spectra of CS powder and pure collagen type II are shown in Fig. 3(a). Using second-derivative analysis, the locations of seven peaks were revealed from the spectra of collagen and CS powders. These peaks were located at ~3195, ~3250, ~3345, ~3450, ~3500, ~3640, and ~3660 cm⁻¹, respectively [Fig. 3(b)]. Among these peaks, both collagen and CS spectrum shared the same peaks located at ~3195, ~3345, and ~3660 cm⁻¹. The peaks at ~3250, ~3450, and ~3640 cm⁻¹ were exclusively associated with collagen, whereas the only peak associated exclusively with CS was located at ~3500 cm⁻¹ [Fig. 3(b)]. Importantly, the peaks identified for pure collagen II and CS were in close agreement with those identified for the organic matrix of native cartilage [Fig. 2(b)].

Gradual hydration of collagen and CS powders from moistened to solvated and then fully hydrated conditions, respectively, allowed observation of the emergence of bound and mobile water fractions. Our results suggested that collagen-bound water-related peaks were located at ~3450 and ~3640, whereas PG-bound water-related peaks were located at ~3500 and ~3660 cm⁻¹, respectively [Figs. 3(c) and 3(d)]. Furthermore, the peaks at ~3195 and ~3345 cm⁻¹ emerged from both collagen- and PG-bound water [Figs. 3(c) and 3(d)]. Continued rehydration of collagen and CS reached equilibrium [Figs. 3(e) and 3(f)]. We calculated 3450/3250 cm⁻¹ ratio that was recently reported as an indicator of water bonding states in skin³³ [Figs. 3(g) and 3(h)]. This value decreased for moistened collagen type II and CS standards compared with baseline but then increased with further rehydration [Figs. 3(g) and 3(h)], indicating a possible translation for water bonding states from bound to mobile during gradual hydration.³³

4 Discussion

Raman OH stretch band of cartilage originates from water molecules (bound and mobile water), the hydroxyl groups of organic matrix macromolecules (i.e., collagen and PG), contributions from NH stretch band, and interactions between these bonds. All these components create one broadband extending

between 3100 and 3800 cm⁻¹, which is similar to spectrum of liquid water [Fig. 1(a)].

Although vibrational [Raman and infrared (IR)] spectroscopy of liquid water has been an active research field for the decades,^{34–40} there is still no consensus on the identities of subbands within the OH-stretch band. Locations of subbands are generally determined by deconvolution, and they are reported to be located at ~3005 to 3015, ~3200 to 3220, ~3400 to 3430, ~3550 to 3570, and ~3600 to 3650^{34–40} depending on temperature, pressure, instrument calibration as well as the deconvolution process. These peak locations are in general agreement with those we identified using the second-derivative method [Fig. 1(b) and Table 1].

OH-subbands are affected by the number of hydrogen bonds,⁴¹ hydrogen-bond bending angles,³⁶ type of the hydrogen bond (e.g., single, bifurcated, or trifurcated),³⁷ the length of hydrogen bond,^{38,39} and the nature of the donor and acceptor configurations of the associated hydrogen bonds.^{39,40,42} A strong hydrogen bonding results in longer bond length; thus, lower wavenumber. Peaks located at lower wavenumber (~3015 and 3220 cm⁻¹) are related to water molecules with stronger hydrogen bonds, while the peaks located at higher frequency (~3400 and ~3565 cm⁻¹) have weaker hydrogen bonds due to the wider energy gap among the vibration modes.^{39,43,44} The peak at ~3600 is reported to be related to nonhydrogen bonded (“free” or “dangling”) water molecules.^{39,40,42,45}

4.1 Bulk Water Displays Five Subpeaks Located Between 3000 and 3800 cm⁻¹ in the OH-Stretch Region of Cartilage Spectrum

In hydrogen bonding, the proton (donor) interacts with an acceptor that is usually an electronegative atom such as oxygen or nitrogen. Therefore, an individual water molecule can interact with neighboring molecules establishing as few as no hydrogen bonds (dangling) to multiple donor and acceptor bonds^{39,40,42,45} [Fig. 5(c)]. In accordance with previous studies on Raman analysis of liquid water,^{39,40,42,45} the peak at ~3015 cm⁻¹ is associated with single donor–double acceptor (DAA-OH) hydrogen bonds, ~3220 cm⁻¹ is associated with double donor–double acceptor (DDAA-OH) hydrogen bonds, ~3410 is associated with single donor–single acceptor (DA-OH) hydrogen bonds, ~3565 is associated with double donor–single acceptor (DDA-OH) hydrogen bonds,^{39,40,42} and ~3630 cm⁻¹ is associated with free-OH [nonhydrogen-bonded (dangling) OH group]⁴⁵ [see Figs. 4(a) and 4(b) for schematically the hydrogen bonding types of water molecules].

4.2 Majority of Water Type in Cartilage is Mobile Water

Our results revealed that wet cartilage spectrum is dominated by mobile water, accounting for ~95% of total Raman signals and the remaining Raman intensities are associated with bound water and solid matrix macromolecules [Fig. 1(c) and Table 2]. This finding is in agreement with the literature that bound water fraction of cartilage was found to be ~4% of total mass using differential scanning calorimetric (DSC) experiment.⁴⁶ Furthermore, most water fraction in cartilage is mobile water state and has little interaction with the matrix.⁴⁶ High content of mobile water in cartilage explains the general similarity between wet cartilage spectrum and bulk water spectrum. However, there is also difference between bulk water

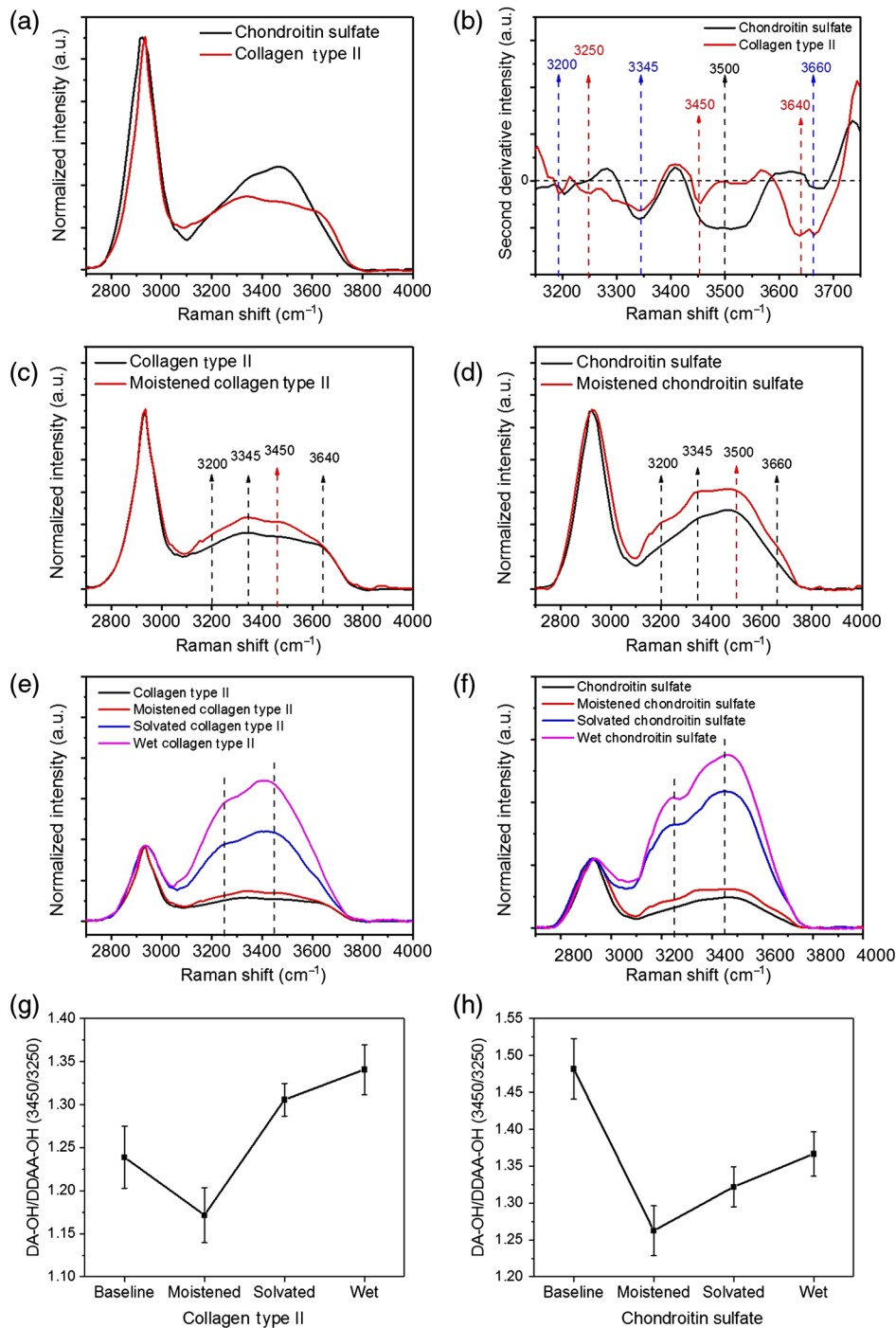


Fig. 3 Raman OH stretching bands of pure collagen type II and CS. (a) Comparison of Raman spectrum of collagen type II and CS. (b) Second derivative spectra of collagen type II and CS. Red dashed lines indicate exclusively collagen-related OH peaks while black dashed lines indicate exclusively PGs-related OH peaks. Blue dashed lines indicate the peaks are associated with both collagen and PGs. (c and d) OH intensity changes of collagen and CS, respectively, after just moistened the samples, showing the peak locations of bound water molecules. (e and f) OH intensity changes of collagen and CS, respectively, during progressive hydration. The standard deviation is within 13% of the intensity and not shown in the spectra for the sake of clarity. (g and h) 3450/3250 Ratio changes of collagen and CS, respectively during progressive hydration.

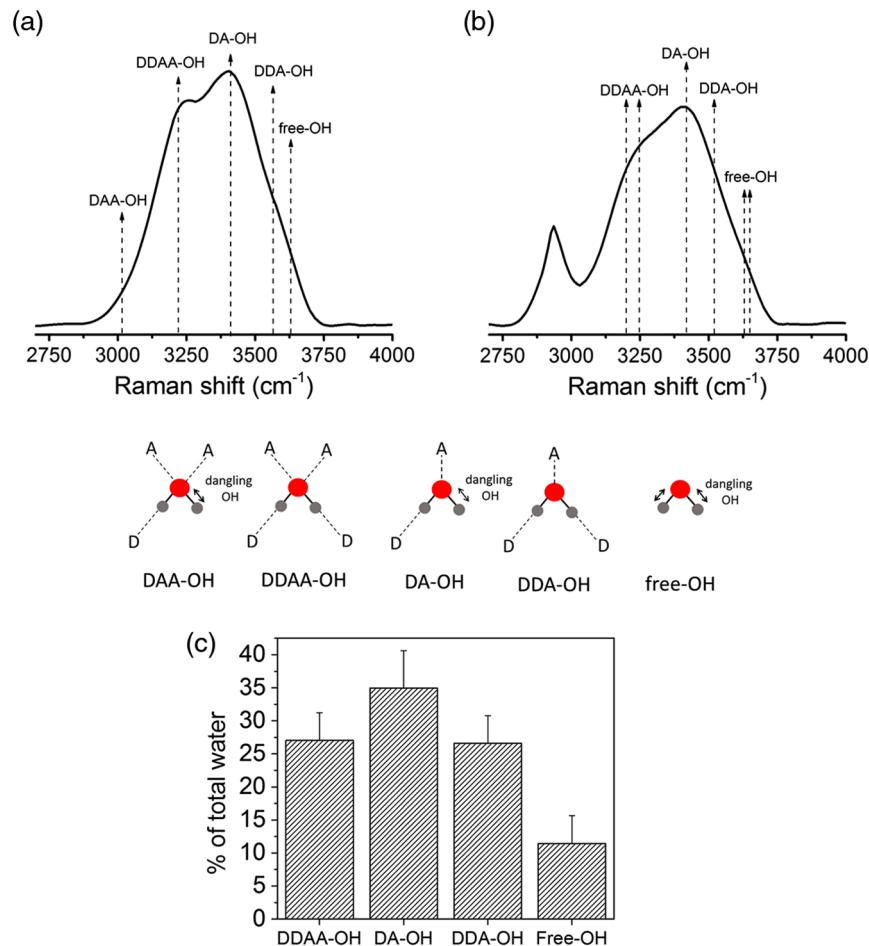


Fig. 4 A schematic depiction of the hydrogen bonding types of water molecules. (a) The Raman OH stretching band of bulk water includes five subpeaks centered at 3015 cm⁻¹ (DAA-OH, single donor–double acceptor), 3220 cm⁻¹ (DDAA-OH, double donor–double acceptor), 3410 cm⁻¹ (DA-OH, single donor–single acceptor), 3565 cm⁻¹ (DDA-OH, double donor–single acceptor), and 3630 cm⁻¹ (free-OH). (b) The Raman OH stretching band of wet cartilage includes six subpeaks centered at 3200 cm⁻¹ (DDAA-OH, double donor–double acceptor), 3250 cm⁻¹ (DDAA-OH, double donor–double acceptor), 3450 cm⁻¹ (DA-OH, single donor–single acceptor), 3500 cm⁻¹ (DDA-OH, double donor–single acceptor), 3630 cm⁻¹, and 3650 cm⁻¹ (free-OH). (c) The percent of water types in cartilage normalized by total water content.

and wet cartilage spectra in that 3250 cm⁻¹ band is less pronounced relative to 3450 cm⁻¹ in cartilage spectrum. This difference may result from the fact that the donor–acceptor interactions are limited to water molecules only in bulk water, whereas additional donor–acceptor interactions occur between water–matrix phases. We further calculated the percent of DDAA-OH, DA-OH, DDA-OH, and free-OH water amount normalized by total water content. As can be seen, the most concentrated water type in the cartilage is DA-OH water molecules (~35%), followed by DDAA-OH and DDA-OH [Fig. 4(c)]. Free-OH water molecules only account for ~10% of total water in cartilage [Fig. 4(c)].

4.3 Peaks Located at 3200 and 3250 cm⁻¹ in Wet Cartilage Spectrum are Associated with DDAA-OH Hydrogen Bonded Water Molecules that are Bound to Collagen and PG (3200 cm⁻¹), and Bound to Specifically Collagen (3250 cm⁻¹) at the State I Hydration Layer

Since it was not possible to distinguish between bound water and mobile water in wet cartilage spectrum, we employed a

sequential dehydration/deuteration as well as a rehydration process to reveal bound water and organic matrix phases. The air drying followed by oven drying at 37°C employed in this study is expected to remove mobile water and has a minimal effect on bound water fraction since removing bound water from the matrix requires temperature at 70°C without denaturation³² or temperatures well in excess of 70°C, which would denature the organic matrix as well.^{47,48} After oven drying for 48 h, we observed the weight of cartilage stabilized. The long-term deuterium exchange beyond oven drying provides information on the rate of dissociation of different moieties of bound water through observation of the disappearance of subpeaks. Overall, our sequential water removal protocol allowed the interpretation of the locations of Raman bands associated with varying water fractions.

In the past, based on DSC experiments, researchers found that there are up to five discrete water fractions observed around collagen structure reportedly ranging from low (state I) to high (state V) concentration.^{49–51} The first hydration shell (state I) corresponds to tightly bound water and state V corresponds to bulk water.^{49–51} To interpret molecular origins of the subpeaks in cartilage, we followed the findings of these DSC studies.^{49–51}

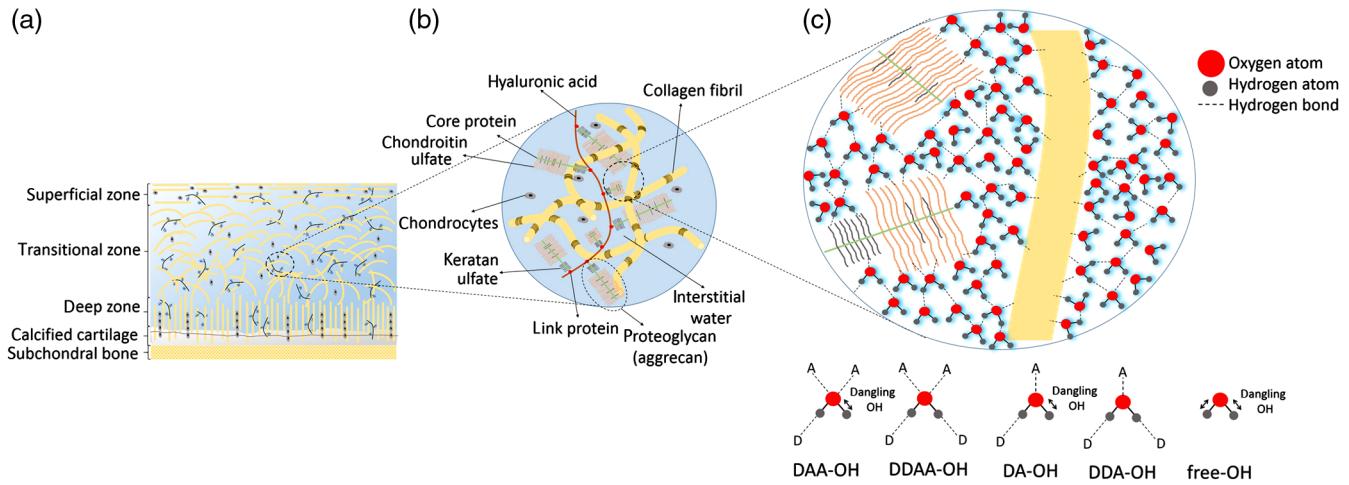


Fig. 5 A schematic depiction of cartilage structure and composition, and hydration layers surrounding collagen fibrils and PGs in the water environment. (a) Illustration of cartilage, (a) structure, and (b) composition. (c) Illustration of the interaction of collagen fibrils and PGs with an individual water molecules establishing as few as no hydrogen bonds (dangling) to multiple donor and acceptor bonds (e.g., DDAA-OH, DA-OH, or DDA-OH). This interaction most likely creates the first hydration layer surrounding to collagen fibrils and PGs, which represents tightly bound water in cartilage. Then, other water molecules bind to these bound water molecules and to each other with the schema of different hydrogen bonds network [e.g., DDAA-OH, DA-OH, DDA-OH or Free-OH (dangling)], creating other water states around the collagen fibrils and PGs, and results an increase in the intensity of corresponding Raman peaks located between 3100 and 3800 cm^{-1} .

As elucidated, peaks in the range of ~ 3200 to $\sim 3250\text{ cm}^{-1}$ in wet cartilage spectrum are assigned as DDAA-OH hydrogen-bonded water molecules^{39,40,42,45} [Fig. 4(b)]. These water molecules have stronger hydrogen bonds and shorter bond lengths compared with DAA-OH, DDA-OH, or DA-OH. Our findings (Figs. 2 and 3) along with the help of the earlier calorimetric studies^{49–51} suggest that water molecules at $\sim 3200\text{ cm}^{-1}$ in wet cartilage spectrum are likely to establish state level I bonds with collagen and PG as the first hydration shell (Fig. 5) since both pure collagen and PG provide a peak at this frequency [Fig. 3(b) and Table 1] and the peak at $\sim 3195\text{ cm}^{-1}$ is observed in deuterated cartilage spectrum [Fig. 2(b)]. Other water molecules may start to bind to state level I molecules and to each other creating other water state levels (e.g., levels II, III, IV, or V) around the organic matrix (Fig. 5), resulting in the sequential increase of the intensity at ~ 3200 and $\sim 3250\text{ cm}^{-1}$ upon hydration of type II collagen and CS [Figs. 3(e) and 3(f)]. It is likely that the band at $\sim 3250\text{ cm}^{-1}$ establishes another set of level I hydrogen bonding network with collagen as evidenced build-up of intensity of this band for collagen [Figs. 3(c) and 3(e)], but not for CS [Figs. 3(d) and 3(f)].

4.4 Peak Located at 3450 cm^{-1} in Wet Cartilage Spectrum is Associated with DA-OH Hydrogen-Bonded Water Molecules that are Bound to Collagen (Hydroxyproline) at the State I Hydration Layer

The peak at 3450 cm^{-1} is assigned as DA-OH hydrogen-bonded water molecules [Fig. 4(b) and Table 1], these water molecules have weaker hydrogen bonds and taller bond lengths compared with DDAA-OH, and thus they are moderately hydrogen bound water molecules. Our findings show that the origin of this peak is associated with collagen molecules [Fig. 3(b)]. More

specifically, the origin of the peak at 3450 cm^{-1} is the hydroxyl group of hydroxyproline according to our previous molecular dynamic simulation of single amino acid chain.²⁷ Briefly, we calculated theoretical/computational peak locations between 3000 and 3800 cm^{-1} for proline, hydroxyproline, and Glycine-Proline-Hydroxyproline (Gly-Pro-Hyp) single amino acid chain. The results showed that only hydroxyproline displayed a peak at $\sim 3450\text{ cm}^{-1}$.²⁷ The intensity associated with hydroxyl group of hydroxyproline in the present study only accounts for $\sim 1.5\%$ of total intensity (Table 2), whereas the majority of intensity is associated with DA-OH water molecules (Table 2). Cumulatively, our results suggest that, at state level I, the hydrogen donor atoms of hydroxyproline bind to acceptor oxygen atoms with the schema of DA-OH hydrogen bonds network. Then, other water molecules bind to these bound water molecules and to each other with the schema of DA-OH hydrogen bonds network [Fig. 5(c)], creating other water states around the collagen and results in an increase in the intensity of this peak [Fig. 3(e)].

4.5 Peak Located at 3520 cm^{-1} in Wet Cartilage Spectrum is Associated with DDA-OH Hydrogen-Bonded Water Molecules that are Bound to PG at the State I Hydration Layer

The peak at 3520 cm^{-1} is assigned as DDA-OH hydrogen-bonded water molecules and our results indicate that the origin of this peak at state level I is associated with the PG phase since this peak is only found in the spectra of CS but not in collagen spectra (Fig. 3), as evidenced build-up of intensity of this band for CS [Figs. 3(d) and 3(f)] but not for collagen [Figs. 3(c) and 3(e)]. These water molecules probably have weaker hydrogen bonds and longer bond lengths than those of Raman bands at lower wavenumbers.

4.6 Peaks Located at 3630 and $\sim 3650\text{ cm}^{-1}$ in Wet Cartilage Spectrum are Mostly Associated with Nonhydrogen-Bonded Water Molecules

The subpeaks at ~ 3630 to $\sim 3650\text{ cm}^{-1}$ are assigned as free-OH [nonhydrogen bonded (dangling) OH] water molecules [Fig. 4(b) and Table 1]. These nonhydrogen-bonded water molecules are typically observed in bulk water when donor and acceptor atoms for creation of hydrogen bonds are relatively limited. Although the major intensity of these peaks are associated with nonhydrogen-bonded water molecules, accounting for $\sim 95\%$ of total intensity (Table 2), our results suggest that collagen molecules also contribute to band at $\sim 3630\text{ cm}^{-1}$ at state level I as suggested by the spectrum of pure collagen standard [Fig. 3(a)]. Spectrum of CS standard implies that CS does not contribute to 3630 cm^{-1} band [Fig. 3(b)]. Deuteration showed that organic phase contribution was limited to $\sim 3\%$ of total Raman intensities (Table 2). The origin of this dangling OH vibration at state level I may be associated with hydroxyl groups of amino acids, such as hydroxyproline, serine, or threonine. Although the peak at 3650 cm^{-1} is also assigned as free-OH water molecules [Fig. 4(b) and Table 1], accounting for $\sim 95\%$ of total intensity (Table 2), our results indicate that the origin of this peak at state level I has contributions from both collagen [Figs. 3(b) and 3(c)] and PG [Figs. 3(b) and 3(d)], accounting for $\sim 4\%$ of total intensity (Table 2) and also as reflected by deuterated cartilage spectrum (Fig. 2). The origin of this peak at state I level may be associated with hydroxyl group of certain amino acids and CS that hydrogen atoms most likely create dangling OH vibration rather than creating a hydrogen bond. However, further studies are needed to identify the moieties of collagen and PG to which these peaks are originating from and to which water molecules are attracted. This dangling OH vibration may also originate from DA-OH hydrogen bonds network, where one of the hydrogen atoms is free to create dangling OH vibration [Figs. 4 and 5(c)]. Though we did not observe a peak at 3345 cm^{-1} in wet cartilage spectrum based on second-derivative analysis [Fig. 1(b)], this peak clearly appears after oven drying [Fig. 2(b)], and is associated with the NH-stretching band of both collagen and PG; however, its intensity is also sensitive to dehydration and deuteration [Fig. 2(a)] indicating contributions of OH vibrations as well.

4.7 $3450/3250\text{ cm}^{-1}$ Ratio can be Used to Study on Water Bonding States in Cartilage

Previously, $3450/3250\text{ cm}^{-1}$ ratio (DA-OH/DDAA-OH) was reported as an indicator of water bonding states in polymer⁵² and skin.³³ The lower value of this ratio indicates the increased number of hydrogen bonds between water molecules and biological tissue.³³ Thus, we calculated this ratio for pure collagen type II and CS standards during gradual rehydration [Figs. 3(g) and 3(h)]. Our results showed that this ratio decreased for moistened samples for both collagen type II and CS, compared with baseline [Figs. 3(g) and 3(h)], suggesting that water molecules start to bind to collagen and CS surfaces creating tightly bound water around them during this stage of hydration [Fig. 5(c)]. Continued rehydration of collagen and CS [Figs. 3(e) and 3(f)] caused an increase in this ratio [Figs. 3(g) and 3(h)], suggesting that water molecules start to bind each other, creating mobile water layers around collagen and CS [Fig. 5(c)]. Therefore,

this ratio can be used as an indicator of water bonding states in cartilage.

This present study has limitations. First, we measured water content in cartilage after a single freeze-thaw cycle at -20°C , which could affect the amount of water content because such freeze-thaw cycle was reported to potentially influence the overall material properties of cartilage.⁵³ Thus, it would be better to assess water content in cartilage from fresh samples or samples refrigerated at 4°C in future studies because such storage condition does not affect the overall material properties of cartilage,⁵³ thereby, expecting to not change the amount of water content in cartilage as well. Second, in this study, Raman data were collected from the surface of articular cartilage. Therefore, it is not represented to depth-dependent water distribution in cartilage. Future studies are needed to qualify depth-dependent water distribution in cartilage.

5 Conclusion

For the first time, OH-stretch band in articular cartilage was investigated to identify the water fractions, which are mobile (removable by prolonged drying at low temperature) and bound (removable by deuterium following prolonged drying) to the matrix of articular cartilage. It was found that the OH-stretch band mostly represents mobile water molecules. We identify six peaks in wet Raman spectrum of articular cartilage whose intensities are sensitive to sequential dehydration. OH vibrations at 3200 and 3650 cm^{-1} are associated with both collagen and PG, and water molecules created at peak at 3200 cm^{-1} are the most tightly hydrogen-bonded water molecules whereas the peak at 3650 cm^{-1} is free-OH bonded, the most mobile water molecules in articular cartilage. The peak at 3250 and 3453 , and 3630 cm^{-1} is exclusively associated with collagen and collagen-related water molecules. The peak at 3520 cm^{-1} is solely associated with PG and PG-related water molecules. However, the moieties of collagen and PG to which these water molecules are attracted remain to be elucidated. It may now be possible to assess the water fractions by RS to study on the hydration perspective of cartilage quality as a potential early diagnosis of OA.

Disclosures

Mustafa Unal has no conflict of interest. Ozan Akkus is the president of Wave# LLC.

Acknowledgments

This material was based in part upon work supported the research Grant no. R01AR057812 (OA) from the NIAMS institute of NIH, and partially supported by think [box] at CWRU. Any opinions, findings, and conclusions or recommendations expressed in this material are those of the author(s) and do not necessarily reflect the views of the NIH.

References

1. T. Neogi and Y. Zhang, "Epidemiology of osteoarthritis," *Rheum. Dis. Clin. North Am.* **39**(1), 1–19 (2013).
2. M. Cross et al., "The global burden of hip and knee osteoarthritis: estimates from the global burden of disease 2010 study," *Ann. Rheum. Dis.* **73**(7), 1323–1330 (2014).
3. H. J. Mankin and A. Thrasher, "Water content and binding in normal and osteoarthritic human cartilage," *J. Bone Jt. Surg.* **57**(1), 76–80 (1975).

4. H. J. Mankin et al., "Biochemical and metabolic abnormalities in articular cartilage from osteo-arthritic human hips," *J. Bone Jt. Surg.* **53**(3), 523–537 (1971).
5. S. Saarakkala et al., "Depth-wise progression of osteoarthritis in human articular cartilage: investigation of composition, structure and biomechanics," *Osteoarthritis Cartilage* **18**(1), 73–81 (2010).
6. L. C. Dijkgraaf et al., "The structure, biochemistry, and metabolism of osteoarthritic cartilage: a review of the literature," *J. Oral Maxillofac. Surg.* **53**(10), 1182–1192 (1995).
7. M. Huber, S. Trattng, and F. Lintner, "Anatomy, biochemistry, and physiology of articular cartilage," *Invest. Radiol.* **35**(10), 573–580 (2000).
8. F. Guilak et al., "Mechanical and biochemical changes in the superficial zone of articular cartilage in canine experimental osteoarthritis," *J. Orthop. Res.* **12**(4), 474–484 (1994).
9. A. F. M. Hani et al., "Non-invasive and in vivo assessment of osteoarthritic articular cartilage: a review on MRI investigations," *Rheumatol. Int.* **35**(1), 1–16 (2015).
10. J. M. Mansour, "Biomechanics of cartilage," in *Kinesiology: the Mechanics and Pathomechanics of Human Movement*, pp. 66–79, Wolters Kluwer Health/Lippincott Williams & Wilkins, Philadelphia, Pennsylvania (2003).
11. G. Blumenkrantz and S. Majumdar, "Quantitative magnetic resonance imaging of articular cartilage in osteoarthritis," *Eur. Cell Mater.* **13**(7), 76–86 (2007).
12. C. Ding, F. Cicutini, and G. Jones, "How important is MRI for detecting early osteoarthritis?" *Nat. Clin. Pract. Rheumatol.* **4**(1), 4–5 (2008).
13. M. Padalkar, R. Spencer, and N. Pleshko, "Near infrared spectroscopic evaluation of water in hyaline cartilage," *Ann. Biomed. Eng.* **41**(11), 2426–2436 (2013).
14. L. Rieppo, J. Töyräs, and S. Saarakkala, "Vibrational spectroscopy of articular cartilage," *Appl. Spectrosc. Rev.* **52**(3), 249–266 (2016).
15. Y. Takahashi et al., "Raman spectroscopy investigation of load-assisted microstructural alterations in human knee cartilage: preliminary study into diagnostic potential for osteoarthritis," *J. Mech. Behav. Biomed. Mater.* **31**, 77–85 (2014).
16. R. A. de Souza et al., "Raman spectroscopy detection of molecular changes associated with two experimental models of osteoarthritis in rats," *Lasers Med. Sci.* **29**(2), 797–804 (2014).
17. N. S. J. Lim et al., "Early detection of biomolecular changes in disrupted porcine cartilage using polarized Raman spectroscopy," *J. Biomed. Opt.* **16**(1), 017003 (2011).
18. K. A. Esmonde-White et al., "Fiber-optic Raman spectroscopy of joint tissues," *Analyst* **136**(8), 1675–1685 (2011).
19. P. Matousek and N. Stone, "Development of deep subsurface Raman spectroscopy for medical diagnosis and disease monitoring," *Chem. Soc. Rev.* **45**(7), 1794–1802 (2016).
20. M. Gniadecka et al., "Structure of water, proteins, and lipids in intact human skin, hair, and nail," *J. Invest. Dermatol.* **110**(4), 393–398 (1998).
21. R. Vyumvuhore et al., "Effects of atmospheric relative humidity on stratum corneum structure at the molecular level: ex vivo Raman spectroscopy analysis," *Analyst* **138**(14), 4103–4111 (2013).
22. S. Wessel et al., "Hydration of human nails investigated by NIR-FT-Raman spectroscopy," *Biochim. Biophys. Acta, Protein Struct. Mol. Enzymol.* **1433**(1), 210–216 (1999).
23. I. Siebinga et al., "Age-related changes in local water and protein content of human eye lenses measured by Raman microspectroscopy," *Exp. Eye Res.* **53**(2), 233–239 (1991).
24. N. Bauer et al., "Noninvasive assessment of the hydration gradient across the cornea using confocal Raman spectroscopy," *Invest. Ophthalmol. Visual Sci.* **39**(5), 831–835 (1998).
25. M. Unal and O. Akkus, "Raman spectral classification of mineral- and collagen-bound water's associations to elastic and post-yield mechanical properties of cortical bone," *Bone* **81**, 315–326 (2015).
26. M. Unal, "Classification of bound water and collagen denaturation status of cortical bone by Raman spectroscopy," Doctoral dissertation, Case Western Reserve University (2017).
27. M. Unal, S. Yang, and O. Akkus, "Molecular spectroscopic identification of the water compartments in bone," *Bone* **67**, 228–236 (2014).
28. C. D. Flanagan et al., "Raman spectral markers of collagen denaturation and hydration in human cortical bone tissue are affected by radiation sterilization and high cycle fatigue damage," *J. Mech. Behav. Biomed. Mater.* **75**, 314–321 (2017).
29. M. Unal and O. Akkus, "Assessment of bone quality by novel spectroscopic biomarkers," in *39th Annual Meeting of American Society of Biomechanics*, Columbus, Ohio (2015).
30. T. Sillinger et al., "DSC measurement of cartilage destruction caused by septic arthritis," *J. Therm. Anal. Calorim.* **82**(1), 221–223 (2005).
31. A. M. Jamieson et al., "Thermal and solvent stability of proteoglycan aggregates by quasielastic laser light-scattering," *Carbohydr. Res.* **160**, 329–341 (1987).
32. E. Sobol et al., "Laser reshaping of cartilage," *Biotechnol. Genet. Eng. Rev.* **17**(1), 553–578 (2000).
33. C. Choe, J. Lademann, and M. E. Darwin, "Depth profiles of hydrogen bound water molecule types and their relation to lipid and protein interaction in the human stratum corneum in vivo," *Analyst* **141**(22), 6329–6337 (2016).
34. G. Walrafen, "Raman spectral studies of water structure," *J. Chem. Phys.* **40**, 3249–3256 (1964).
35. G. E. Walrafen, "Raman spectral studies of the effects of solutes and pressure on water structure," *J. Chem. Phys.* **55**(2), 768–792 (1971).
36. R. Rey, K. B. Møller, and J. T. Hynes, "Hydrogen bond dynamics in water and ultrafast infrared spectroscopy," *J. Phys. Chem. A* **106**(50), 11993–11996 (2002).
37. N. Chumavskii and M. Rodnikova, "Some peculiarities of liquid water structure," *J. Mol. Liq.* **106**(2–3), 167–177 (2003).
38. D. A. Schmidt and K. Miki, "Structural correlations in liquid water: a new interpretation of IR spectroscopy," *J. Phys. Chem. A* **111**(40), 10119–10122 (2007).
39. Q. Sun, "The Raman OH stretching bands of liquid water," *Vib. Spectrosc.* **51**(2), 213–217 (2009).
40. U. Buck and F. Huisken, "Infrared spectroscopy of size-selected water and methanol clusters," *Chem. Rev.* **100**(11), 3863–3890 (2000).
41. G. Walrafen, "Raman and infrared spectral investigations of water structure," in *The Physics and Physical Chemistry of Water*, pp. 151–214, Springer, New York (1972).
42. C. Steinbach et al., "Infrared predissociation spectroscopy of large water clusters: a unique probe of cluster surfaces," *J. Phys. Chem. A* **108**(29), 6165–6174 (2004).
43. N. Kitadaï et al., "Effects of ions on the OH stretching band of water as revealed by ATR-IR spectroscopy," *J. Solution Chem.* **43**(6), 1055–1077 (2014).
44. K. Ohno et al., "The effect of cooperative hydrogen bonding on the OH stretching-band shift for water clusters studied by matrix-isolation infrared spectroscopy and density functional theory," *Phys. Chem. Chem. Phys.* **7**(16), 3005–3014 (2005).
45. P. Perera et al., "Observation of water dangling OH bonds around dissolved nonpolar groups," *Proc. Natl. Acad. Sci. U. S. A.* **106**(30), 12230–12234 (2009).
46. V. Bagratashvili et al., "Thermal and diffusion processes in laser-induced stress relaxation and reshaping of cartilage," *J. Biomech.* **30**(8), 813–817 (1997).
47. C. A. Miles et al., "The increase in denaturation temperature following cross-linking of collagen is caused by dehydration of the fibres," *J. Mol. Biol.* **346**(2), 551–556 (2005).
48. Y. Chae et al., "Effect of water content on enthalpic relaxations in porcine septal cartilage," *J. Therm. Anal. Calorim.* **95**(3), 937–943 (2008).
49. M. Pineri, M. Escoubes, and G. Roche, "Water–collagen interactions: calorimetric and mechanical experiments," *Biopolymers* **17**(12), 2799–2815 (1978).
50. A. Haly and J. Snaith, "Calorimetry of rat tail tendon collagen before and after denaturation: the heat of fusion of its absorbed water," *Biopolymers* **10**(9), 1681–1699 (1971).
51. J. Kopp, M. Bonnet, and J. Renou, "Effect of collagen crosslinking on collagen-water interactions (a DSC investigation)," *Matrix* **9**(6), 443–450 (1990).
52. Y. Maeda and H. Kitano, "The structure of water in polymer systems as revealed by Raman spectroscopy," *Spectrochim. Acta, Part A* **51**(14), 2433–2446 (1995).
53. A. Changoor et al., "Effects of refrigeration and freezing on the electro-mechanical and biomechanical properties of articular cartilage," *J. Biomech. Eng.* **132**(6), 064502 (2010).

Mustafa Unal is currently a postdoctoral research fellow at the Department of Orthopaedic Surgery and Rehabilitation at Vanderbilt University Medical Center. He received his PhD in mechanical engineering from Case Western Reserve University in 2017. His research interests include biomedical Raman spectroscopy, bone and cartilage biomechanics, and biomedical diagnostics.

Ozan Akkus is a professor at the Departments of Mechanical and Aerospace Engineering and Biomedical Engineering at Case Western Reserve University. He is a fellow of ASME and AIMBE. His research interests include biomedical diagnostics, Raman spectroscopy, and biofabrication.